Characterization of Mental States through Node Connectivity between Brain Signals

Tiziana Cattai[1,2,3], Stefania Colonnese[3], Marie-Constance Corsi[1,2], Danielle S. Bassett[4,5,6,7], Gaetano Scarano[3], Fabrizio De Vico Fallani[1,2]

[1]*Inria Paris, Aramis project-team, Paris, France*

[2]*Institut du Cerveau et de la Moelle Épinière, ICM, Inserm, U 1127, CNRS, UMR 7225, Sorbonne Université, F-75013, Paris, France*

[3]*Dept. of Information Engineering, Electronics and Telecommunication, Sapienza University,Rome, Italy*

[4]*Department of Bioengineering, University of Pennsylvania, Philadelphia, PA, 19104, USA*

[5]*Department of Electrical and Systems Engineering, University of Pennsylvania, Philadelphia, PA, 19104, USA*

[6]*Department of Physics & Astronomy, University of Pennsylvania, Philadelphia, PA, 19104, USA*

[7]*Department of Neurology, Hospital of the University of Pennsylvania, Philadelphia, PA, 19104, USA*

Corresponding author: fabrizio.devicofallani@gmail.com

***Abstract*—Discriminating mental states from brain signals is crucial for many applications in cognitive and clinical neuroscience. Most of the studies relied on the feature extraction from the activity of single brain areas, thus neglecting the potential contribution of their functional coupling, or connectivity. Here, we consider spectral coherence and imaginary coherence to infer brain connectivity networks from electroencephalographic (EEG) signals recorded during motor imagery and resting states in a group of healthy subjects. By using a graph theoretic approach, we then extract the weighted node degree from each network and evaluate its ability to discriminate the two mental states as a function of the number of available observations. The obtained results show that the features extracted from spectral coherence networks outperform those obtained from imaginary coherence in terms of significant difference, neurophysiological interpretation and reliability with fewer observations. Taken together, these findings suggest that graph algebraic descriptors of brain connectivity networks can be further explored to classify mental states.**

***Index Terms*—EEG, Spectral Coherence, Imaginary Coherence, Weighted Node degree, Motor imagery**

I. Introduction

The ability to distinguish mental states from electroencephalographic (EEG) signals is gaining more and more importance for several noninvasive applications, such as brain-computer interface [1] and biometry [2]. The majority of the studies focused on activity features which characterize single brain regions [3], [4]. However, temporal dependence-based features could be more representative of complex neurophysiological processes, compared to activity of each brain area separately [5].

Functional connectivity measures the dependence between the activity of different brain areas, reflecting information exchanges that are crucial to understand brain organization. There is an increasing interest in devising novel connectivity estimators [6] to quantify functional interaction between brain regions [7], possibly adopting a signal processing on graph perspective [8] to describe EEG signals in time, frequency, as well as in novel transform domains such as the Slantlet domain [9] or the graph spectral domain [10], [11]. Among other state-of-the-art connectivity metrics, the spectral coherence as well as its imaginary counterpart, the imaginary coherence, are well-assessed estimators describing the synchronization in amplitude between signals [12], [13]. The main difference between the coherence and the imaginary coherence is that this latter neglects components that are instantaneously estimated at all the EEG electrodes due to a smearing effect on the scalp caused by the conductibility of cerebral tissues (volume conduction effect) [14].

Here, we study different connectivity-based features to discriminate between motor imagery and resting states. Specifically, we study i) the spectral coherence and imaginary coherence between the EEG signals; ii) the weighted node degrees of the brain network graphs built on the above estimates [15], [16]. Finally, we apply the proposed approaches on high-density EEG signals recorded in a group of healthy subjects during motor-imagery and resting states, and we statistically evaluate their relative ability in separating the two mental states.

II. Functional connectivity estimators

N signal samples are acquired at frequency F_s in two different mental states, S_1 and S_2. Samples are obtained from M EEG-electrodes for each state, collecting T_{S1}

ISBN 978-90-827970-1-5

trials in S_1 and T_{S2} trials in S_2; the procedure is repeated for I subjects.

The signal Acquisition Stage (AS) in S_1 and S_2 states for the i-th user, t-th trial, m-th channel, n-th signal sample yields the real measurements' sets:

$$X^{(S_1)} = \{x_m^{(i,t)}[n]\},\ S_1\ \text{AS}\} \tag{1}$$

$$X^{(S_2)} = \{x_m^{(i,t)}[n]\},\ S_2\ \text{AS}\} \tag{2}$$

For both the ASs, the following power spectral estimates are computed:

$$P_{x_m}^{(i,t)}[k] = \frac{1}{L_W}\sum_{l=0}^{L_W}\left|\sum_{n=0}^{N-1} w_l[n]x_m^{(i,t)}[n]e^{-j2\pi nk/N}\right|^2 \tag{3}$$

$$P_{x_{m_1}x_{m_2}}^{(i,t)}[k] = \frac{1}{L_W}\sum_{l=0}^{L_W}\left(\sum_{n=0}^{N-1} w_l[n]x_{m_1}^{(i,t)}[n]e^{-j2\pi nk/N}\right)\cdot \left(\sum_{n=0}^{N-1} w_l[n]x_{m_2}^{(i,t)}[n]e^{-j2\pi nk/N}\right)^* \tag{4}$$

where $w_l[n]$, with $l = 0,\cdots L_W - 1$ and $n = 0,\cdots N-1$ is a suitable set of L_W real windows, depending on the estimation method. For instance, the MultiTaper method [17] adopts a set of sinusoidal functions of duration N, whereas the Welch method adopts a set of time orthogonal functions [18].

We use two estimators to understand the relation between couples of signals, i.e. the spectral coherence and imaginary coherence, defined as follows:

$$C_{m1\,m2}^{(i,t)}[k] = \frac{\left|P_{x_{m_1}x_{m_2}}^{(i,t)}[k]\right|}{\left(P_{x_{m_1}}^{(i,t)}[k]\cdot P_{x_{m_2}}^{(i,t)}[k]\right)^{1/2}} \tag{5}$$

$$IC_{m1\,m2}^{(i,t)}[k] = \frac{\left|\Im\left(P_{x_{m_1}x_{m_2}}^{(i,t)}[k]\right)\right|}{\left(P_{x_{m_1}}^{(i,t)}[k]\cdot P_{x_{m_2}}^{(i,t)}[k]\right)^{1/2}} \tag{6}$$

Spectral coherence is a well established estimator used in literature [19]. Imaginary coherence has the theoretical advantage of eliminating connectivity at lag 0, [14] that can be originated by the smearing of the EEG signals on the scalp caused by the different electrical conductibility of brain tissues. As shown in Fig. 1, spectral coherence is generally higher and more sensitive to short-distance connections than imaginary coherence. In the following section we adopt a graph theoretical approach to derive compact description of the inferred EEG connectivity networks in the two mental states S_1 and S_2.

III. Proposed Algebraic Descriptor

A graph $G = (V,E)$, consists of two sets V and E, such that $V \neq \emptyset$ and E is a set of pairs of elements of V. The elements of $V = (v_1, v_2, ..., v_n)$ are the vertices (or nodes) of G, while the elements of $E = (e_1, e_2, ..., e_n)$ are its edges (or links) [20]. In our case, the nodes represent EEG electrodes and their connections are weighted by the connectivity estimators (spectral coherence and imaginary coherence). In this section, we use the weighted node degree as a compact index of the connectivity of each electrode [16].

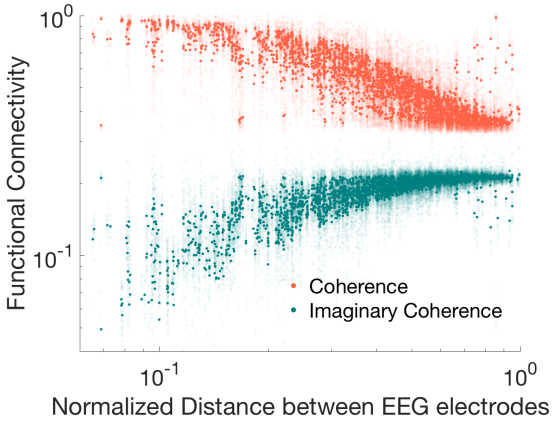

Fig. 1: Behavior of connectivity estimators as a function of distance between EEG electrodes. Results are pooled from all the available experimental observations in the B_{beta} frequency band as described in following section.

Specifically, we consider the Coherence-based Node Degree (CND) and Imaginary Coherence-based Node Degree (ICND), defined as follows:

$$\text{CND}_m^{(i,t)} = \frac{1}{||B||}\sum_{k\in B}\sum_{c=0}^{M-1} C_{m\,c}^{(i,t)}[k] \tag{7}$$

$$\text{ICND}_m^{(i,t)} = \frac{1}{||B||}\sum_{k\in B}\sum_{c=0}^{M-1} IC_{m\,c}^{(i,t)}[k] \tag{8}$$

where B denotes the set of frequency indexes selected for the evaluation and $||.||$ denotes the cardinality of the set.

We then compute the trial-averaged Coherence based Node Degree statistic under the two mental states:

$$\overline{CND}_m^{(i)}\Big|_{S_i} = \left\{\frac{1}{T}\sum_{t=0}^{T-1}\text{CND}_m^{(i,t)},\ S_i\ \text{AS}\right\} \tag{9}$$

and the trial-averaged Imaginary Coherence based Node Degree:

$$\overline{ICND}_m^{(i)}\Big|_{S_i} = \left\{\frac{1}{T}\sum_{t=0}^{T-1}\text{ICND}_m^{(i,t)},\ S_i\ \text{AS}\right\} \tag{10}$$

Similarly, we define the corresponding measures for coherence and imaginary coherence, namely the trial-

ISBN 978-90-827970-1-5 © EURASIP 2018

averaged Link Coherence

$$\overline{C}^{(i)}_{m_1\,m_2}\Big|_{S_i} = \left\{ \frac{1}{T}\sum_{t=0}^{T-1} \frac{1}{||B||}\sum_{k\in B} C^{(i,t)}_{m1\,m2}[k],\ S_i \text{ AS} \right\} \quad (11)$$

and the trial-averaged Link Imaginary Coherence

$$\overline{IC}^{(i)}_{m_1\,m_2}\Big|_{S_i} = \left\{ \frac{1}{T}\sum_{t=0}^{T-1} \frac{1}{||B||}\sum_{k\in B} IC^{(i,t)}_{m1\,m2}[k],\ S_i \text{ AS} \right\} \quad (12)$$

Our goal is to discriminate between the two mental states, taking into consideration the above graph descriptors. In the following section, we evaluate their discriminant ability.

IV. Experimental results

The above methods are tested on EEG data recorded in a group of 10 healthy subjects, all right handed. During the experiment, a subject is in front of a screen, displaying a target: when the target is up, the subject is instructed to perform a motor imagery (MI) task with the right hand (i.e. grasping) and when the target is down, she/he should just rest. The recording session consists in 5 runs of 32 trials (or epochs) each, 16 of MI and 16 of resting. Each trial lasts 5 s; this is the temporal window used for the connectivity inference procedure. EEG signals are recorded with frequency sampling of 1 kHz and then downsampled to 250 Hz. We consider 74 electrodes in a standard 10-10 configuration. The obtained signals are pre-processed to identify and remove artifacts associated to blinks or cardiac activity. An independent component analysis (ICA) [21] based on *Infomax* algorithm [22] is realized with Fieldtrip toolbox [23] and each component, along with its associated topography is visually analyzed.

After ICA, we evaluate the defined metrics, where S_1 corresponds to MI, and S_2 to resting state; the number of subjects is $I = 10$, electrodes are $M = 74$ and trials are $T = 74$ per condition. For the spectral estimation the Welch method with Hanning window of 1 s and 50% of overlap is used [18]. We compute functional connectivity and connectivity-based node degree in the two conditions MI and resting state. We then average the results into four frequency bands: $B_{theta} = 4-7$Hz, $B_{alpha} = 8-13$Hz, $B_{beta} = 14-29$Hz and $B_{gamma} = 30-40$Hz.

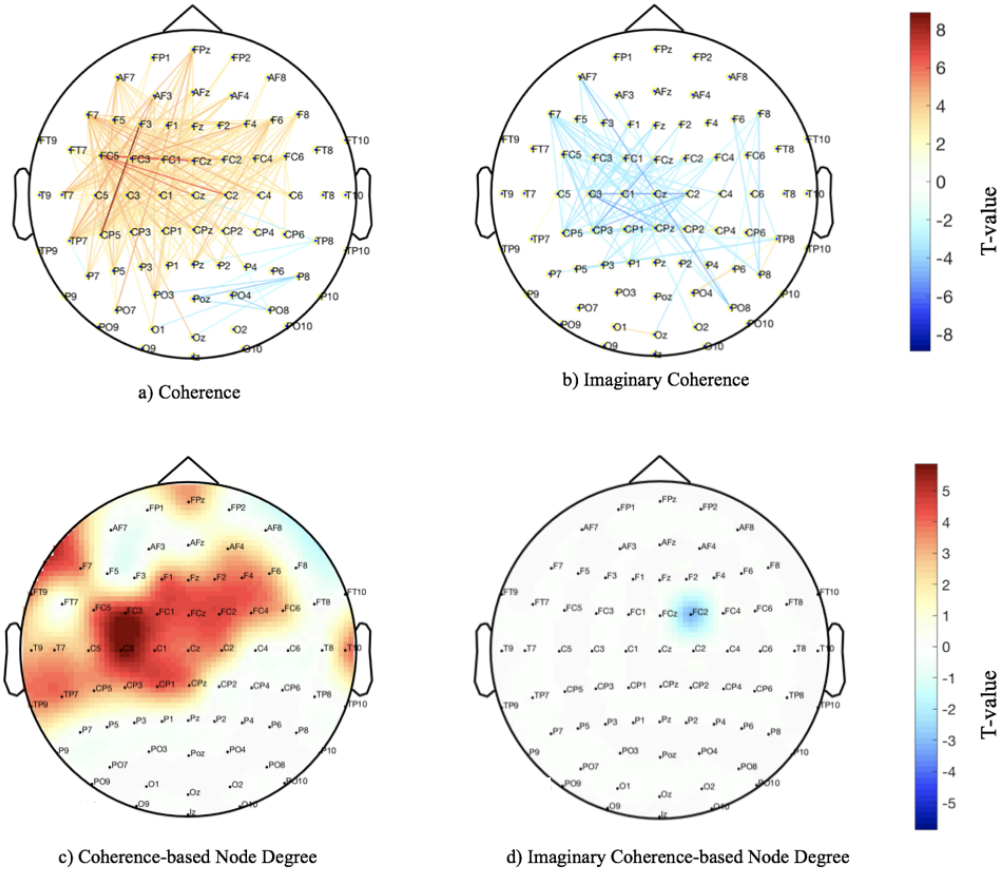

Fig. 2: t-value maps resulting from the difference between MI and resting states in the B_{beta} band.

ISBN 978-90-827970-1-5 © EURASIP 2018

Finally, for each frequency band, we perform a statistical test to quantify the discriminant ability of the metrics in the following way:

- In the case of coherence and imaginary coherence, for each possible couple of channels $m1 - m2$, we collect the correspondent connectivity values in MI and resting for the ten subjects;
- For connectivity-based node degree, for each channel m we collect the metric values for MI and rest for each subject.

Considering the difficulty of performing a classification test with only 10 subjects, we decided to use a statistical test, which describes the discriminative potential of the features. In fact, in both the cases, a paired permutation test is performed, using *resampling statistical toolkit*, with significance level $\alpha = 0.05$, corrected for multiple comparisons with False Discovery Rate. The discriminant capability of the metrics is measured by the t-value, which is proportional to the average, evaluated across subjects, of the connectivity metrics difference among the two conditions.

In Fig. 2, we report the results of the t-tests according to the different metrics, with t-values filtered out by non significant corrected p-values. These results refer to the B_{beta} band, which is the one with the highest significant differences.

For comparison's sake, we considered the t-test according to the power spectral estimate, traditional feature in EEG signals. To this end, we repeated the same analysis with the averaged $P_{x_m}^{(i,t)}[k]$ across trials and across frequencies in B_{beta} band for each channel m. Results showed a decrease in the motor area, that is associated to non significant values, in particular the t-value varies in a range between -1.74 and 1.38. These findings suggest that connectivity features are more stable than power spectrum across subjects in the same frequency band.

Carrying on with the analysis of connectivity estimators, in Beta band, coherence-based features have higher t-values compared to imaginary coherence-based ones. Moreover, in Fig. 2a,c, the increase is localized in connections involving the controlateral motor areas (ie, left hemisphere, FC, C, CP electrodes). In the following we only report the results obtained with coherence and coherence-based node degree. In particular, we study the obtained t-values as a function of the number of trials: we start with all trials ($T = 74$) and decrease them until $T = 5$.

We consider the coherence-based node degree of the channel with the largest t-value, C3, and compare its performance with respect to the link with the strongest coherence, Cp5-F3. In Table I, we notice that the weighted node degree of the node C3 has a lower t-value with a great number of trials. Decreasing the number of observations, it remains higher than the t-value of the single connection. These results highlight the resilience capability of coherence-based node degree, which tends to discriminate mental states even with a reduced number of trials. In Fig. 3, we finally report a generic progressive decrease of t-values for the electrodes in left central hemisphere as a function of the number of trials.

TABLE I: T-values for Coherence-based Node Degree in C3 and Coherence in between Cp5-F3

Table T-value	*Number of Trials* 74	66	59	51	43	36	28	20	13	5
T-value C3	5.861	5.663	5.863	4.951	3.361	2.383	2.649	2.818	2.221	1.412
T-value Cp5-F3	8.867	7.338	7.956	4.645	2.794	2.279	2.386	2.464	1.852	1.427

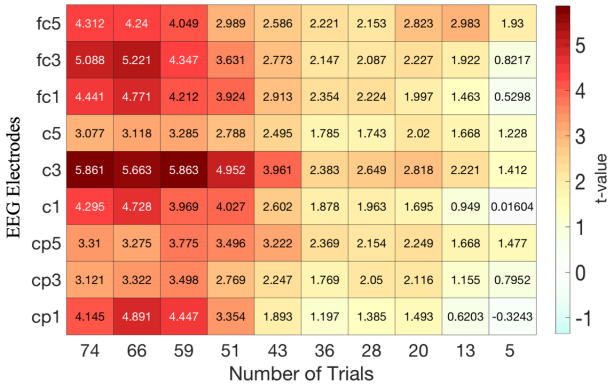

Fig. 3: t-values for the coherence-based node degree in the B_{beta} band for central electrodes as a function of the number of trials.

We report in Table II, for the sake of completeness, the highest t-values for coherence-based node degree in other frequency bands.

TABLE II: Maximum t-values for Coherence-based Node Degree in other Frequency Bands

Table T-value	*Coherence-based Node degree* Theta Band	Alpha Band	Beta Band	Gamma Band
T-max	2.25	2.01	5.861	2.19

V. Conclusion and Further Work

Graph analysis of functional brain networks offers a compact and powerful tool to characterize the complex interactions of EEG signals [16]. Here, we

ISBN 978-90-827970-1-5 © EURASIP 2018

compare the performance of two popular connectivity estimators in inferring networks whose topological local properties could separate motor imagery and resting states. The obtained results show that spectral coherence-based node degrees in the B_{beta} frequency band give stronger differences compared to imaginary coherence ones (Fig. 2). In particular, we report a coherent connectivity increase around the C3 electrode, which corresponds to the motor cortex contralateral to the movement and which is typically involved during motor related tasks [24], [25]. We speculate that this result could be in part explained by the fact that imaginary coherence causes the elimination of contributions at lag 0, which can instead possibly carry relevant neurophysiological information [26]. Finally, compared to simple connectivity measures, coherence-based node degrees are more resilient to decrease of available observations (trials) needed to infer the EEG connectivity networks (Table I, Fig. 3). This in an important feature, as in many clinical/cognitive applications, such as brain-computer interfaces [27], [28] the detection of mental states must be performed on-line to ensure optimal man-machine interaction. Taken together, these results pave the way for leveraging node connectivity descriptors for several applications based on mental states discrimination.

REFERENCES

[1] K. Moxon and G. Foffani, "Brain-machine interfaces beyond neuroprosthetics," *Neuron*, vol. 86, no. 1, pp. 55 – 67, 2015.

[2] D. La Rocca, P. Campisi, B. Vegso, P. Cserti, G. Kozmann, F. Babiloni, and F. D. V. Fallani, "Human brain distinctiveness based on eeg spectral coherence connectivity," *IEEE transactions on Biomedical Engineering*, vol. 61, no. 9, pp. 2406–2412, 2014.

[3] F. Lotte, L. Bougrain, and M. Clerc, "Electroencephalography (eeg)-based brain–computer interfaces," *Wiley Encyclopedia of Electrical and Electronics Engineering*, 2015.

[4] P. Herman, G. Prasad, T. M. McGinnity, and D. Coyle, "Comparative analysis of spectral approaches to feature extraction for eeg-based motor imagery classification," *IEEE Transactions on Neural Systems and Rehabilitation Engineering*, vol. 16, no. 4, pp. 317–326, 2008.

[5] M. Billinger, C. Brunner, and G. R. Müller-Putz, "Single-trial connectivity estimation for classification of motor imagery data," *Journal of neural engineering*, vol. 10, no. 4, p. 046006, 2013.

[6] G. Karanikolas and G. Giannakis, "Identifying directional connections in brain networks via multi-kernel granger models," in *Acoustics, Speech and Signal Processing (ICASSP), 2017 IEEE International Conference on*, pp. 6304–6308, IEEE, 2017.

[7] L. Shaw and A. Routray, "Topographical pattern analysis using wavelet based coherence connectivity estimation in the distinction of meditation and non-meditation eeg," in *Signal Processing Conference (EUSIPCO), 2017 25th European*, pp. 1554–1558, IEEE, 2017.

[8] L. Goldsberry, W. Huang, N. Wymbs, S. Grafton, D. Bassett, and A. Ribeiro, "Brain signal analytics from graph signal processing perspective," pp. 851–855, 2017.

[9] A. K. Ibrahim, H. Zhuang, N. Erdol, and A. M. Ali, "Eeg seizure detection by integrating slantlet transform with sparse coding," in *Signal Processing Conference (EUSIPCO), 2017 25th European*, pp. 459–462, IEEE, 2017.

[10] W. Huang, L. Goldsberry, N. Wymbs, S. Grafton, D. Bassett, and A. Ribeiro, "Graph frequency analysis of brain signals," *IEEE Journal on Selected Topics in Signal Processing*, vol. 10, no. 7, pp. 1189–1203, 2016.

[11] F. Grassi, A. Loukas, N. Perraudin, and B. Ricaud, "A time-vertex signal processing framework: Scalable processing and meaningful representations for time-series on graphs," *IEEE Transactions on Signal Processing*, vol. 66, no. 3, pp. 817–829, 2018.

[12] D. J. Krusienski, D. J. McFarland, and J. R. Wolpaw, "Value of amplitude, phase, and coherence features for a sensorimotor rhythm-based brain–computer interface," *Brain research bulletin*, vol. 87, no. 1, pp. 130–134, 2012.

[13] Q. Wei, Y. Wang, X. Gao, and S. Gao, "Amplitude and phase coupling measures for feature extraction in an eeg-based brain–computer interface," *Journal of Neural Engineering*, vol. 4, no. 2, p. 120, 2007.

[14] G. Nolte, O. Bai, L. Wheaton, Z. Mari, S. Vorbach, and M. Hallett, "Identifying true brain interaction from eeg data using the imaginary part of coherency," *Clinical neurophysiology*, vol. 115, no. 10, pp. 2292–2307, 2004.

[15] F. D. V. Fallani, F. Pichiorri, G. Morone, M. Molinari, F. Babiloni, F. Cincotti, and D. Mattia, "Multiscale topological properties of functional brain networks during motor imagery after stroke," *Neuroimage*, vol. 83, pp. 438–449, 2013.

[16] F. D. V. Fallani, J. Richiardi, M. Chavez, and S. Achard, "Graph analysis of functional brain networks: practical issues in translational neuroscience," *Phil. Trans. R. Soc. B*, vol. 369, no. 1653, p. 20130521, 2014.

[17] K. S. Riedel and A. Sidorenko, "Minimum bias multiple taper spectral estimation," *IEEE Transactions on Signal Processing*, vol. 43, no. 1, pp. 188–195, 1995.

[18] P. Welch, "The use of fast fourier transform for the estimation of power spectra: a method based on time averaging over short, modified periodograms," *IEEE Transactions on audio and electroacoustics*, vol. 15, no. 2, pp. 70–73, 1967.

[19] G. C. Carter, "Coherence and time delay estimation," *Proceedings of the IEEE*, vol. 75, no. 2, pp. 236–255, 1987.

[20] M. Newman, *Networks: an introduction*. Oxford university press, 2010.

[21] A. Delorme, T. Sejnowski, and S. Makeig, "Enhanced detection of artifacts in eeg data using higher-order statistics and independent component analysis," *Neuroimage*, vol. 34, no. 4, pp. 1443–1449, 2007.

[22] A. J. Bell and T. J. Sejnowski, "An information-maximization approach to blind separation and blind deconvolution," *Neural computation*, vol. 7, no. 6, pp. 1129–1159, 1995.

[23] R. Oostenveld, P. Fries, E. Maris, and J.-M. Schoffelen, "Fieldtrip: open source software for advanced analysis of meg, eeg, and invasive electrophysiological data," *Computational intelligence and neuroscience*, vol. 2011, p. 1, 2011.

[24] G. Pfurtscheller and A. Aranibar, "Event-related cortical desynchronization detected by power measurements of scalp eeg," *Clinical Neurophysiology*, vol. 42, no. 6, pp. 817–826, 1977.

[25] G. Pfurtscheller, "Spatiotemporal erd/ers patterns during voluntary movement and motor imagery," in *Supplements to Clinical neurophysiology*, vol. 53, pp. 196–198, Elsevier, 2000.

[26] R. Vicente, L. L. Gollo, C. R. Mirasso, I. Fischer, and G. Pipa, "Dynamical relaying can yield zero time lag neuronal synchrony despite long conduction delays," *Proceedings of the National Academy of Sciences*, vol. 105, no. 44, pp. 17157–17162, 2008.

[27] J. R. Wolpaw, N. Birbaumer, D. J. McFarland, G. Pfurtscheller, and T. M. Vaughan, "Brain–computer interfaces for communication and control," *Clinical neurophysiology*, vol. 113, no. 6, pp. 767–791, 2002.

[28] I. Daly, S. J. Nasuto, and K. Warwick, "Brain computer interface control via functional connectivity dynamics," *Pattern recognition*, vol. 45, no. 6, pp. 2123–2136, 2012.

ISBN 978-90-827970-1-5 © EURASIP 2018